



Alexandria University  
**Alexandria Engineering Journal**

[www.elsevier.com/locate/aej](http://www.elsevier.com/locate/aej)  
[www.sciencedirect.com](http://www.sciencedirect.com)



# A computational study on mixed convection in a porous media filled and partially heated lid-driven cavity with an open side

Nidal H. Abu-Hamdeh <sup>a,b,\*</sup>, Hakan F. Oztop <sup>c,b</sup>, Khalid A. Alnefaie <sup>b</sup>

<sup>a</sup> Center of Research Excellence in Renewable Energy and Power Systems, King Abdulaziz University, Jeddah 21589, Saudi Arabia

<sup>b</sup> Mechanical Engineering Department, Faculty of Engineering, King Abdulaziz University, Jeddah 21511, Saudi Arabia

<sup>c</sup> Department of Mechanical Engineering, Technology Faculty, Firat University, Elazig, Turkey

Received 16 October 2019; revised 18 March 2020; accepted 28 April 2020

Available online 4 June 2020

## KEYWORDS

Lid-driven cavity;  
 Porous;  
 Open cavity;  
 Partial heating;  
 Finite volume technique

**Abstract** Applications of mixed convection due to lid-driven cavities can be found in different engineering technologies. A computational study was conducted to explore the effects of different parameters on mixed convection in a porous media filled lid-driven cavity with one side opening in the presence of heat generation. The cavity has a flush mounted heater on its bottom wall. The governing equations were solved by developing a computer code by using finite volume technique for different parameters as length of heater (1/5, 2/5, 4/5), Richardson number (0.1, 1, 10) and Darcy number (0.1, 0.01, 0.001). It is found that heat transfer and flow field inside the cavity is so complex due to moving lid, open side wall and heater. Heat transfer increases with increasing of Grashof numbers, heater length and decreased with Darcy numbers.

© 2020 The Authors. Published by Elsevier B.V. on behalf of Faculty of Engineering, Alexandria University. This is an open access article under the CC BY-NC-ND license (<http://creativecommons.org/licenses/by-nc-nd/4.0/>).

## 1. Introduction

Mixed convection due to lid-driven cavities can be find applications in different engineering technologies such as moving belts near objects, cooling of electronical equipments, ocean engineering and automotive engines. The media can be pure air, water, nanofluid or porous media. Convection associated with porous media has been investigated extensively in the past few decades due to its numerous engineering applications [1–3].

\* Corresponding author.

E-mail address: [nabuhamdeh@kau.edu.sa](mailto:nabuhamdeh@kau.edu.sa) (N.H. Abu-Hamdeh).

Peer review under responsibility of Faculty of Engineering, Alexandria University.

<https://doi.org/10.1016/j.aej.2020.04.039>

1110-0168 © 2020 The Authors. Published by Elsevier B.V. on behalf of Faculty of Engineering, Alexandria University.

This is an open access article under the CC BY-NC-ND license (<http://creativecommons.org/licenses/by-nc-nd/4.0/>).

Most of the studied systems in engineering have finite length heater such as house heating systems, electronic equipments or local heating systems. In this perspective, a reviewal work was made by Oztop et al. [4] to show the applications of partial heating for different systems. Ahmed et al. [5] analysed the natural convection including radiation heat transfer in a partially heated cavity. Oztop et al. [6] investigated the natural convection in a partially opened porous cavity. They found that increasing the porosity of the cavity's interior increases the heat transfer rate. They also deduced that there are an optimum opening location for each value of porosity. Chung and Vafai [7] researched the effect of vibration on the heat convection in an open-ended porous enclosure. The opening in their study is at the top. They found that increasing the vibration of the left wall resulted in enhanced heat transfer.



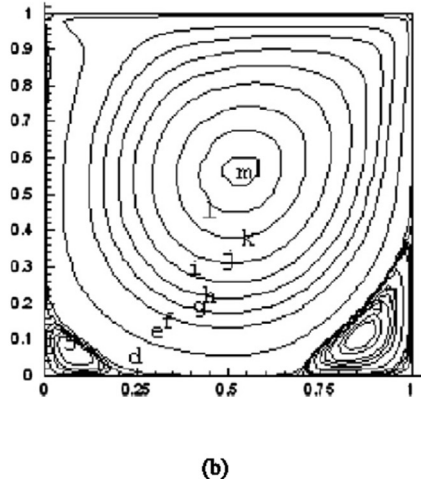
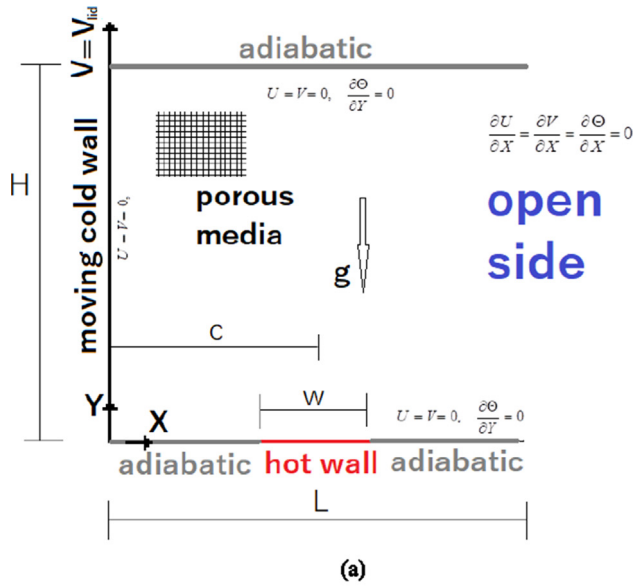


Fig. 1 (a) Physical Model, (b) Streamlines for  $Re = 1000$  for validation.

Table 3 Mean Nusselt number comparison between literature and this study for  $Da = 0.1$ .

$Ri$	$\overline{Nu}(present)$	$Nu$ [29]	% deviation
0.1	4.196	3.92	6.5
1	2.312	2.31	0
5	1.746	1.83	4.5

Table 4 Comparison of mean Nusselt numbers with literature studies from ref. Oztop [30].

Study	Results
Baytas [31]	3.160
Saeid and Pop [32]	3.002
Present	2.980

Table 5 Verification of the streamfunction values with literature [37,38].

Present study	Refs. [37,38]
d	$-0.92 \times 10^{-4}$
e	-0.0061
f	-0.025
g	-0.039
h	-0.053
i	-0.08
J	-0.094
k	-0.103
l	-0.108
m	-0.11

Table 1 Source term as given in Eq. (1) (Oztop [9]).

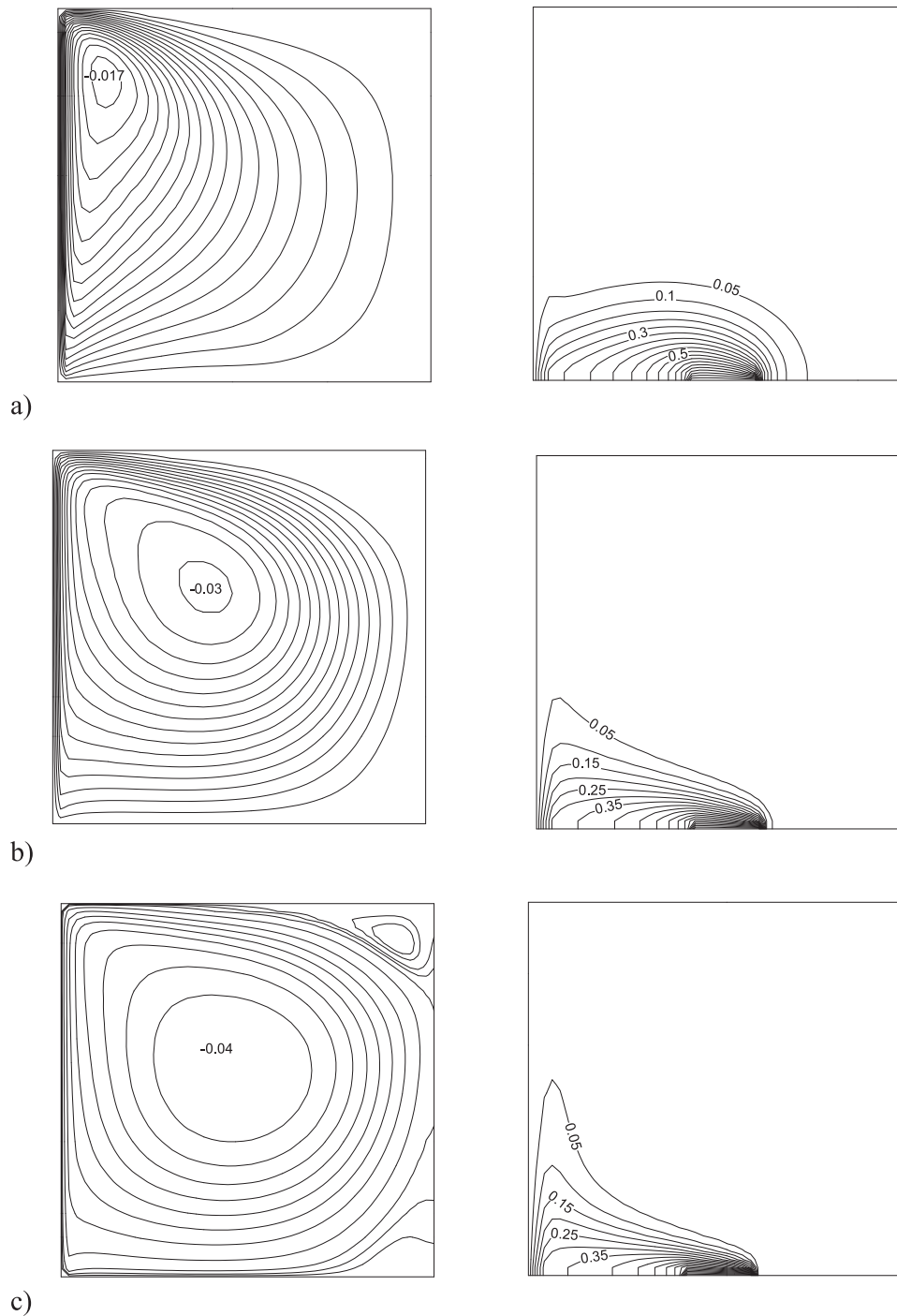
Equation	S
Continuity	0
x-momentum	$-\varepsilon^{+2} \frac{\partial p}{\partial X} + \frac{\partial}{\partial X} \Gamma \frac{\partial U}{\partial X} + \frac{\partial}{\partial Y} \Gamma \frac{\partial V}{\partial X} - U \left\{ \frac{\Gamma}{K/\varepsilon} + \frac{C_F}{(K/\varepsilon)^{1/2}} (U^2 + V^2)^{1/2} \right\}$
y-momentum	$-\varepsilon^{+2} \frac{\partial p}{\partial Y} + \frac{\partial}{\partial X} \Gamma \frac{\partial U}{\partial Y} + \frac{\partial}{\partial Y} \Gamma \frac{\partial U}{\partial Y} + \varepsilon^{+2} \frac{Gr}{Re^2} T - V \left\{ \frac{\Gamma}{K/\varepsilon} + \frac{C_F}{(K/\varepsilon)^{1/2}} (U^2 + V^2)^{1/2} \right\}$

Table 2 Validation of results.

Porosity	$Gr$	Haghshenas et al. [29]	Present study	% deviation
$\varepsilon = 0.4$	$Gr = 10^4$	1.541	1.498	2.7
	$Gr = 10^5$	4.294	4.010	6.5
	$Gr = 10^6$	9.432	8.86	6.0
$\varepsilon = 0.6$	$Gr = 10^4$	1.731	1.689	2.4
	$Gr = 10^5$	5.032	4.867	3.2
	$Gr = 10^6$	11.211	10.631	5.1

medium filling a lid-driven square enclosure for both non-uniform and uniform heating. They found that low values but almost uniform local Nusselt numbers for low Peclet numbers. They found also, for high Peclet numbers at  $Da = 10^{-3}$ , localized enhancement for heat transfer rates. Other related studies on natural convection or mixed convection heat transfer and fluid flow under different boundary conditions can be found in refs.

In this study, the case is such that one vertical side of an open sided cavity moves and the cavity has a partial heater. The novelty of the present work that it presents the application of a moving lid heated cavity with open sided filled partially with porous media. Different governing parameters were analyzed to investigate their effects on heat and fluid flow in the case described.



**Fig. 2** Streamlines (on the left) and isotherms (on the right) for different Darcy numbers,  $Re = 1000$ ,  $Gr = 10^5$ ,  $x_L/L = 1/5$  and  $c/H = 1/5$ , (a)  $Da = 0.001$ , (b)  $Da = 0.01$ , (c)  $Da = 0.1$ .

2. Physical model

Fig. 1 shows the complete model of the two-dimensional flow model along with the coordinates and the boundary condi-

tions. The enclosure is a square one with the length  $L = H$ . In addition it moves with constant velocity, the top wall of the cavity has isothermal boundary conditions with temperature lower than the corners's heater temperature. The lengths of

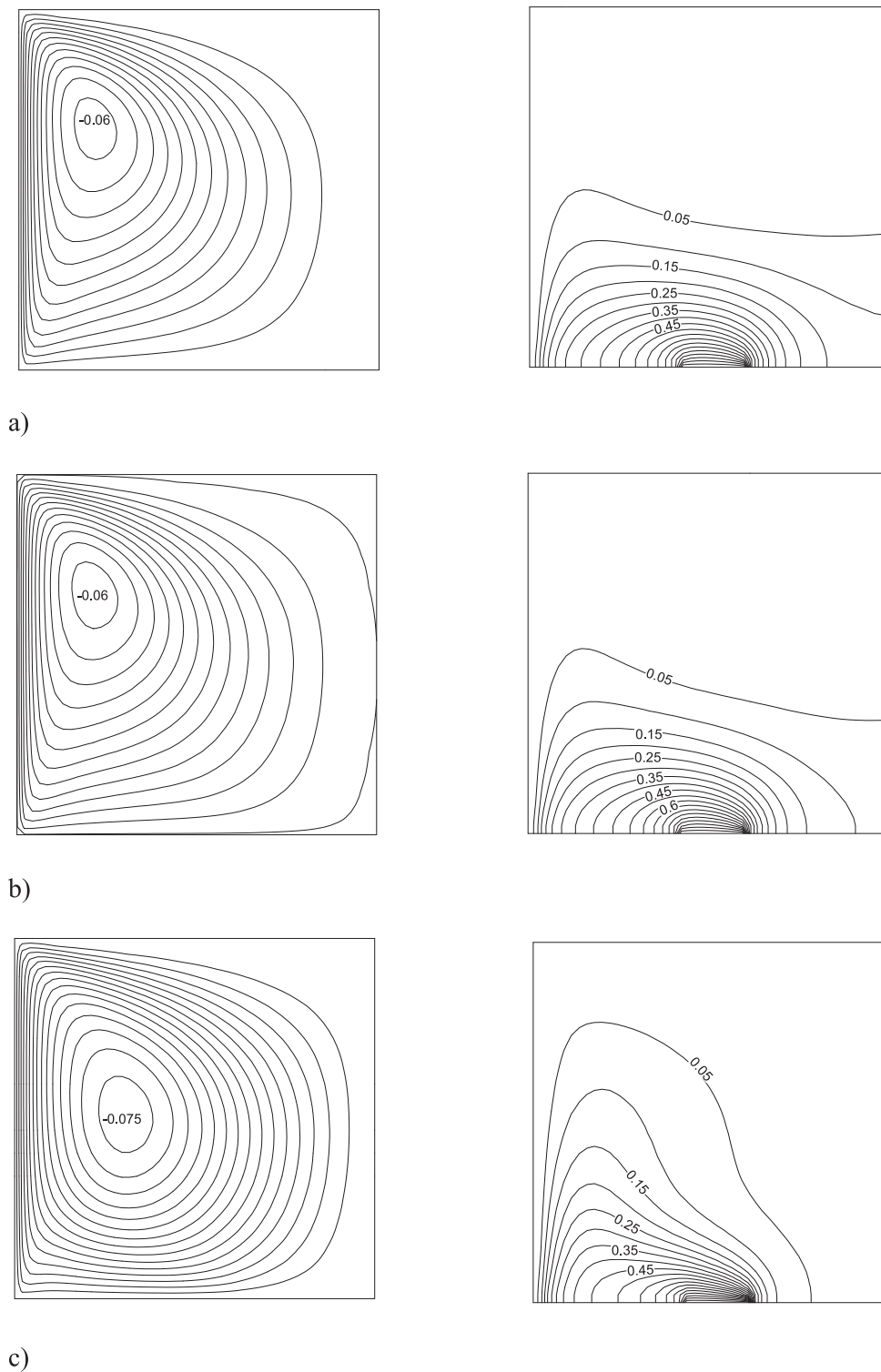


Fig. 3 Streamlines (on the left) and isotherms (on the right) for different Darcy numbers,  $Re = 100$ ,  $Da = 0.01$ ,  $x_L/L = 1/5$  and  $c/H = 1/5$ , (a)  $Gr = 10^3$ , (b)  $Gr = 10^4$ , (c)  $Gr = 10^5$ .

the isothermal boundaries of the corner heater in the horizontal and vertical directions are  $XH$  and  $YH$ , respectively.

### 3. Governing equations

Assumptions can be listed as

- The walls are impermeable and adiabatic.
- It is valid to use Boussinesq approximation.

- Radiation is neglected compared to other heat transfer modes.
- The gravity acts towards the earth's center ( $-y$  direction).

The following is the governing equation in dimensional form [9]:

$$\frac{\partial}{\partial X} \left( U\phi - \Gamma \frac{\partial \phi}{\partial X} \right) + \frac{\partial}{\partial Y} \left( V\phi - \Gamma \frac{\partial \phi}{\partial Y} \right) = S \tag{1}$$

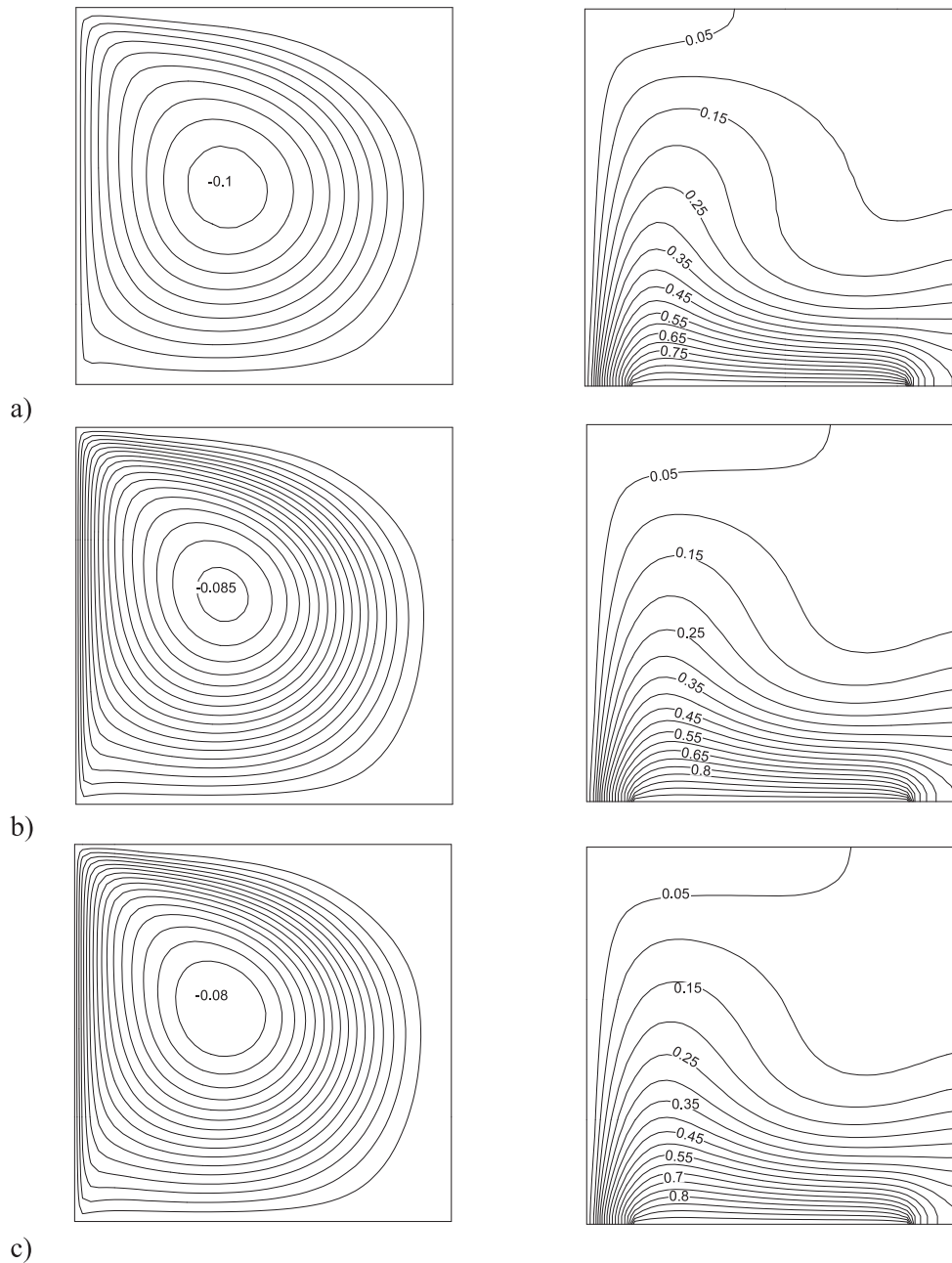


**Fig. 4** Streamlines (on the left) and isotherms (on the right) for different Darcy numbers,  $Da = 0.1$ ,  $Re = 1000$ ,  $Gr = 10^5$ ,  $x_L/L = 1/5$  and  $c/H = 1/5$ , (a)  $Gr = 10^5$ , (b)  $Gr = 10^4$ , (c)  $Gr = 10^3$ .



Source term  $S$  is given in Table 1. Dimensionless parameters are also given as follows:

$$\begin{aligned}
 X &= \frac{x'}{H}, & Y &= \frac{y'}{H}, & U &= \frac{u'}{V_{lid}}, & V &= \frac{v'}{V_{lid}}, & P &= \frac{p'}{\rho V_{lid}^2}, & \Theta &= \frac{T' - T_c}{T_h - T_c}, \\
 Da &= \frac{K}{H^2}, & Gr &= \frac{CK^{3/2}g\beta\Delta TH^3}{\nu^2}, & Re &= \frac{V_{lid}H}{\nu}, & Ri &= \frac{Gr}{Re^2}, & Pr &= \frac{\nu}{\alpha}
 \end{aligned}
 \tag{2}$$

3.1. Boundary conditions

The boundary conditions in this study are shown on the physical model of the geometry as in Fig. 1. The solid walls' boundary conditions were no-slip. A 0.9 porosity ( $\epsilon$ ) was assumed. The pertinent boundary conditions are given as follows

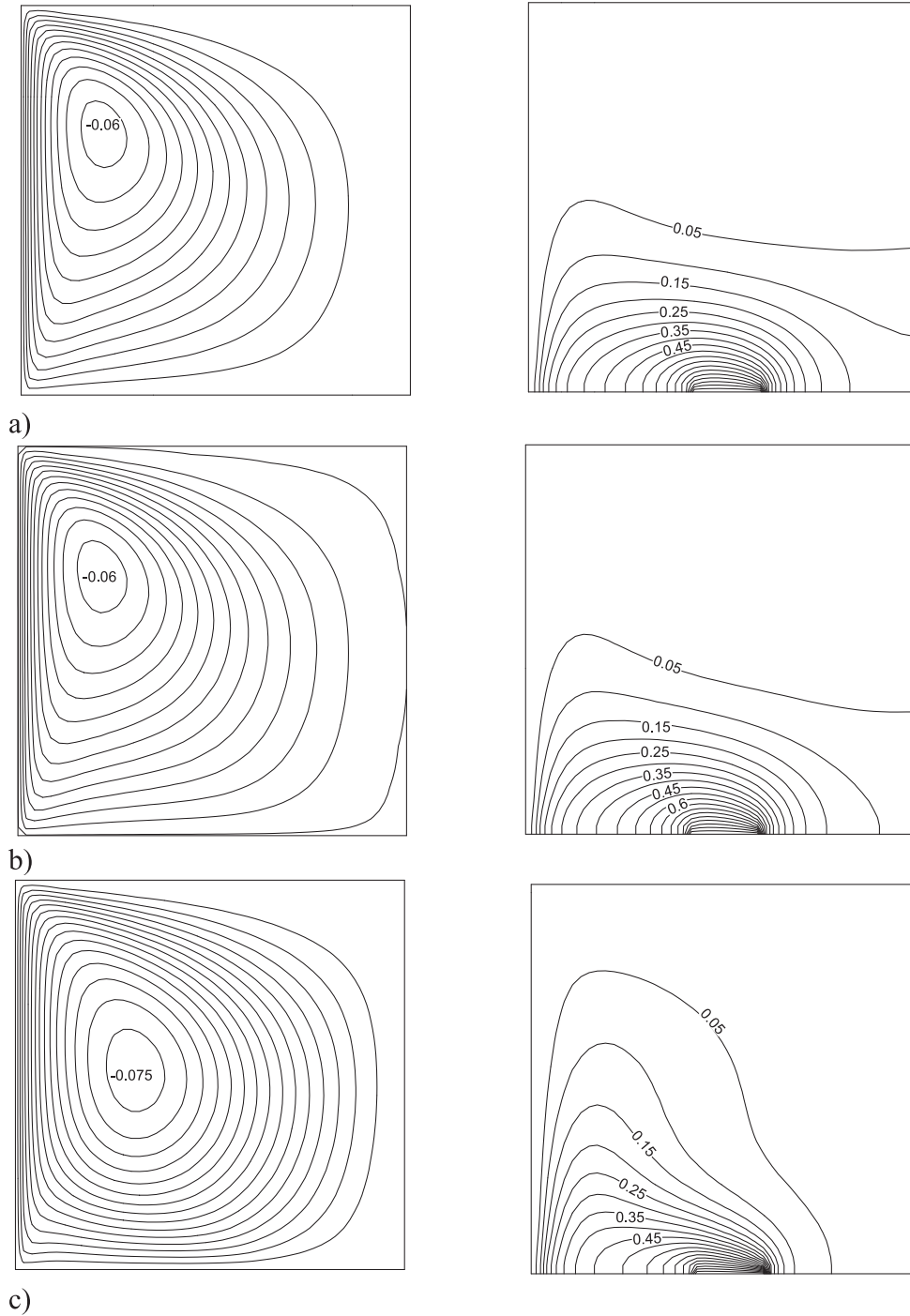


Fig. 5 Streamlines (on the left) and isotherms (on the right) for different Darcy numbers,  $Re = 100$ ,  $Da = 0.01$ ,  $w/L = 1/5$  and  $c/H = 1/5$ , (a)  $Gr = 10^3$ , (b)  $Gr = 10^4$ , (c)  $Gr = 10^5$ .

at top wall :  $Y = H, \quad 0 < X < L, \quad U = V = 0, \quad \frac{\partial \Theta}{\partial Y} = 0$  (3a)

at bottom wall  $Y = 0, \quad 0 \leq X \leq L, \quad U = V = 0, \quad \frac{\partial \Theta}{\partial Y} = 0$  (3b)

along the heater  $\Theta = 1$  (3c)

at left wall  $X = 0, \quad 0 \leq Y \leq H, \quad U = \Theta = 0, \quad V = 1$  (3d)

at right wall  $X = L, \quad 0 \leq Y \leq H, \quad \frac{\partial U}{\partial X} = \frac{\partial V}{\partial X} = \frac{\partial \Theta}{\partial X} = 0$  (3e)

The local Nusselt  $Nu_x$  and average Nusselt numbers are the physical quantities of interest. They are calculated along the hot wall as

$$Nu_x = -\left(\frac{\partial \Theta}{\partial y}\right)_{X=w} \quad (4)$$

$$\overline{Nu} = \int_{w=0}^w Nu_x dy \quad (5)$$

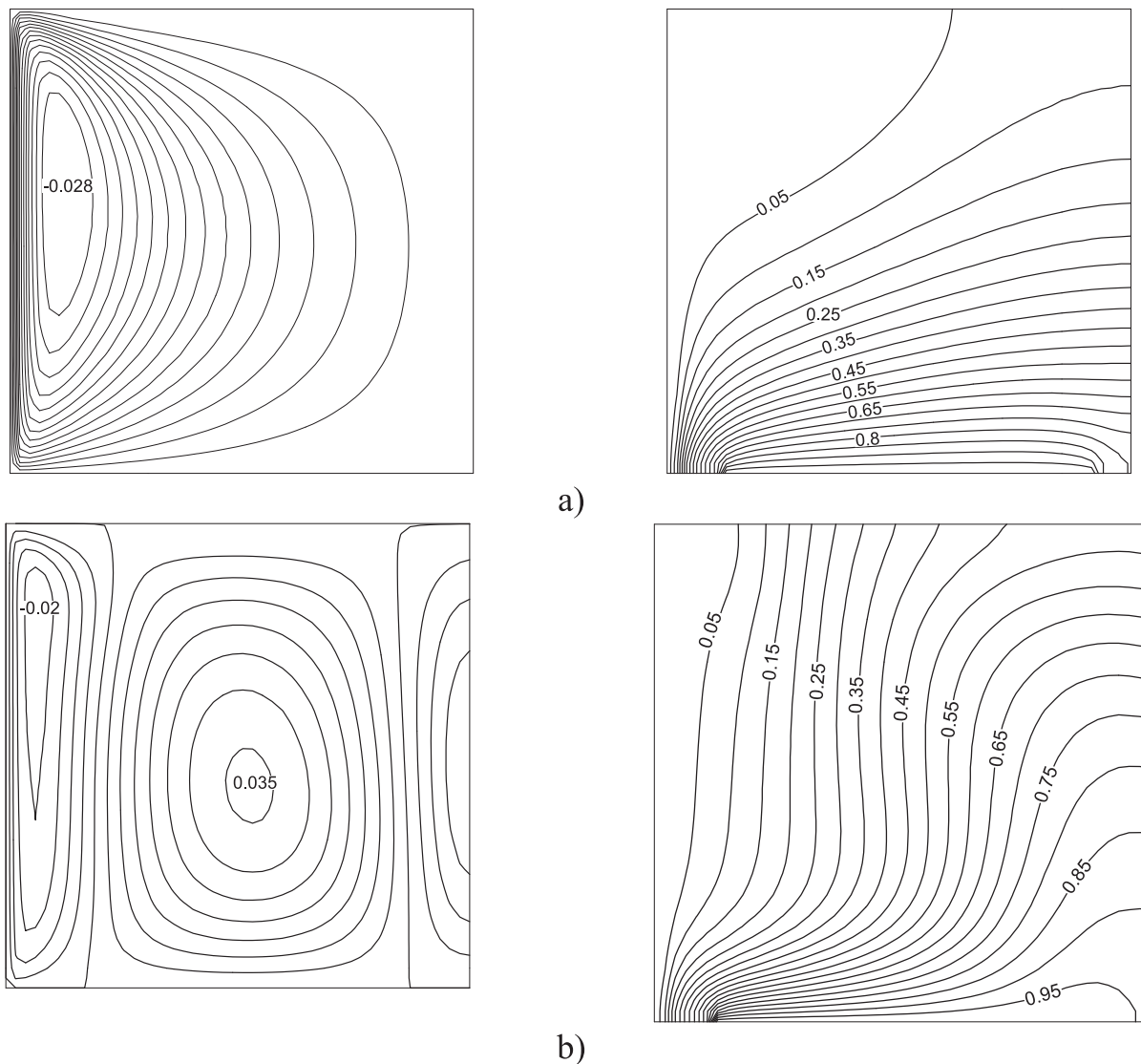


**Fig. 6** Streamlines (on the left) and isotherms (on the right) for different Darcy numbers,  $Re = 100, Da = 0.001, w/L = 4/5$  and  $c/H = 0.5$ , (a)  $Gr = 10^3$ , (b)  $Gr = 10^5$ .



3.2. Validation and grid test

A test was performed and the results obtained were used to validate the code with those found in literature. The obtained results are shown in Table 2. There was a good agreement between the Haghshenas et al. [33] results and the present test results. The authors are not aware of any related experimental data for comparison with the numerical results shown in Table 3 and Table 4. Other validation results for the studied code can be found in refs. [9,18,51-36]. Fig. 1 (b) and Table 5 show the qualitative validation from refs. [37,38]. The comparison shows that the results are acceptable.

In order to solve the governing equation, an arrangement of staggered grid was used in the finite difference method that is based on finite volume. Nakayama [28] proposed a modified version of the general purpose of SAINTS code which was used with SIMPLE algorithm [27]. The SAINTS stands to

an integration of turbulence and porous media simulator with Navier–Stokes equation. A hybrid of upwind schemes and the central difference was used for the diffusive and convective terms. The TDMA method was used to solve the linear algebraic equation. The definition of the stream function was used to calculate it as  $u = \partial\psi/\partial y$ ,  $v = \partial\psi/\partial x$ . To obtain a solution’s stable convergence of v-velocity, u-velocity, pressure and energy equations, an under-relaxation parameter of 0.3, 0.3, 0.2 and 0.5 were used. In the computational solution, grids dimension tested were  $24 \times 24$ ,  $36 \times 36$  and  $48 \times 48$ . Based on the results obtained, the 48x48 dimension was chosen for the meshing the grid. Next to the boundaries, fine grids were used in the mesh.

Satisfying the following condition was used to terminate the iteration process:

$$\sum_{ij} \left| \Phi_{ij}^m - \Phi_{ij}^{m-1} \right| / \sum_{ij} \left| \Phi_{ij}^m \right| < 10^{-5} \tag{6}$$

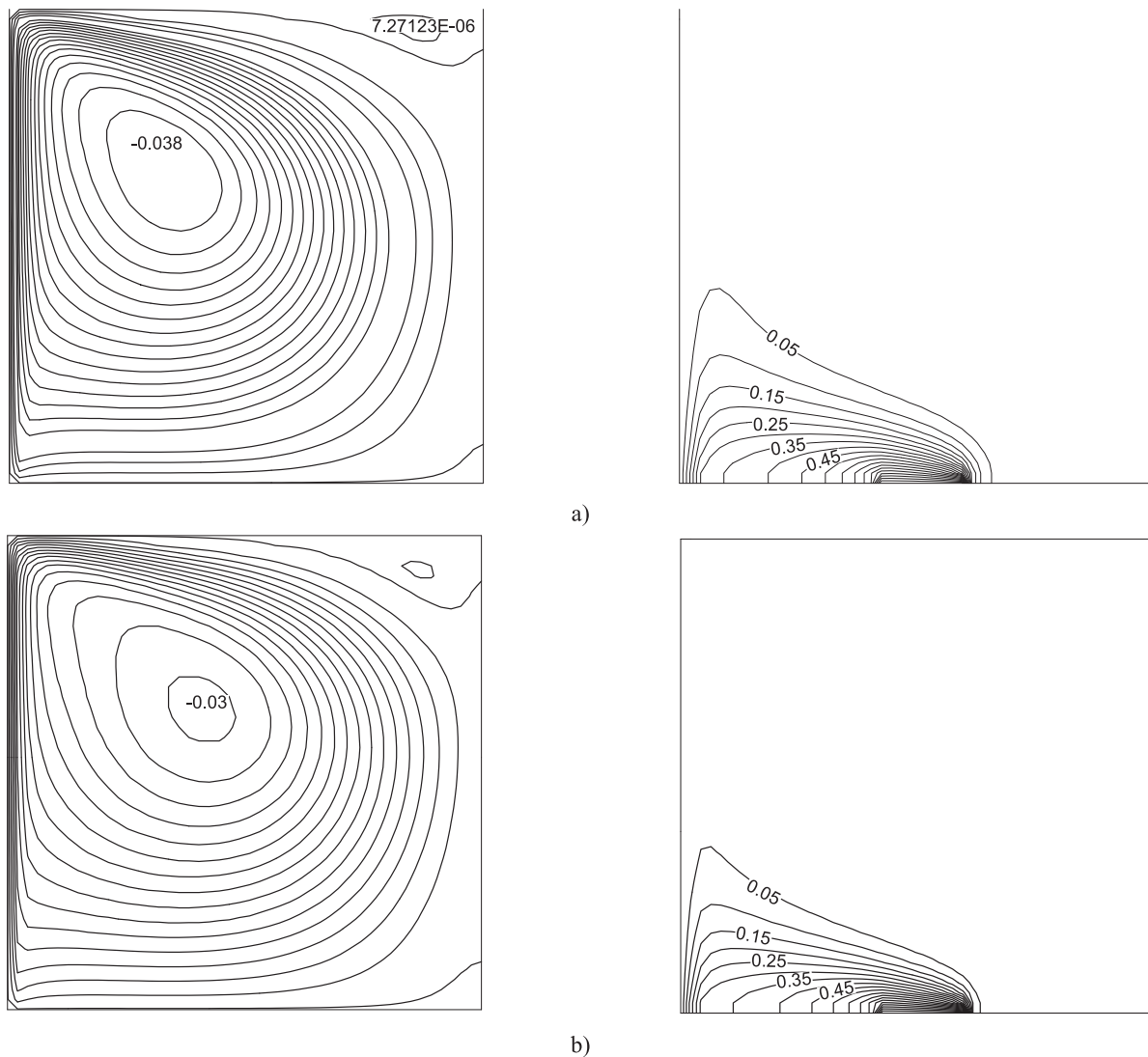


Fig. 7 Streamlines (on the left) and isotherms (on the right) for different Reynolds numbers,  $Da = 0.001$ ,  $c/H = 0.5$  and  $w/L = 1/5$ ,  $Gr = 10^5$ . (a)  $Re = 500$ , (b)  $Re = 1000$ .

where U stands for either V, U, P or dimensionless temperature and m implies the iteration step.

### 4. Results and discussion

This computational work of a partially heated porous media filled open cavity with left side moving wall at different parameters as length of partial heating ( $1/5 \leq w/L \leq 1$ ), ( $0.3 \leq c/L \leq 0.7$ ) location of heater, Grashof numbers ( $10^3 \leq Gr \leq 10^5$ ), Reynolds number ( $100 \leq Re \leq 1000$ ) and Darcy number ( $0.001 \leq Da \leq 0.1$ ). Based on these parameters, the results will be presented as isotherms, streamlines, mean and local Nusselt numbers, temperature variations and velocity distribution. For higher Grashof number such as  $Gr = 10^6$ , the code did not work due to oscillation or transition to turbulent. Thus, the results are presented for lower than this value for safety in all cases.

Fig. 2 shows the isotherms (on the right) and the streamlines (on the left) for different Darcy numbers at  $Re = 1000$ ,  $Gr = 10^5$ ,  $w/L = 1/5$  and  $c/H = 0.5$ . A clockwise circulation cell is formed for all Darcy numbers except  $Da = 0.1$ . A formation of small circulation cell nearby the right top side based on stream function values was noticed; flow strength increased with increasing Darcy numbers. The center of main cell moves diagonally with increasing of Darcy number. Its shape is also a function of Darcy number. Fig. 3 shows isotherms (on the right) and streamlines (on the left) for parameters of  $Re = 100$ ,  $Da = 0.01$ ,  $w/L = 1/5$  and  $c/H = 0.5$  at different Grashof numbers. Both temperature distribution and flow field are not affected at lower Grashof numbers because of the conduction mode dominates the other modes of heat transfer. On the contrary, as seen from isotherms which are presented in right column, conduction mode turns to be prevailing at lower values of Grashof number. For  $Ri = 1$  ( $Ri = Gr/Re^2$ ), most of

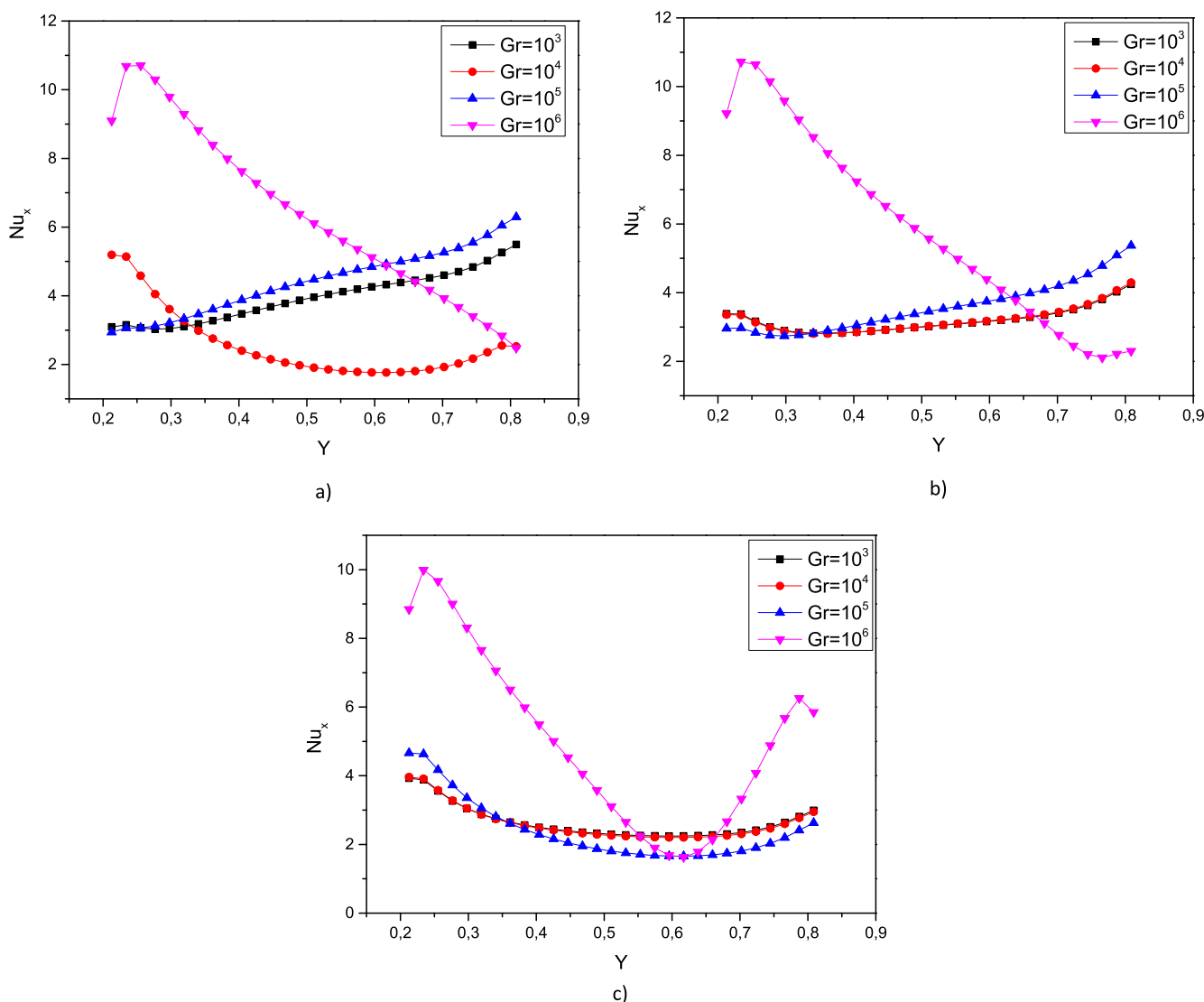


Fig. 8 Variation of local Nusselt number along the heater for different Grashof numbers at  $Re = 100$ ,  $c/H = 0.5$  and  $w/L = 1/5$ , (a)  $Da = 0.1$ , (b)  $Da = 0.01$ , (c)  $Da = 0.001$ .

the fluid becomes same temperature and little plume is observed near the moving lid as seen from Fig. 3(b). As shown in Fig. 3(c), as Grashof number increases natural convection becomes dominant. Fig. 4 illustrates the isotherms (on the right) and streamlines (on the left) for different Grashof numbers and parameters of  $Da = 0.1$ ,  $Re = 1000$ ,  $Gr = 10^5$ ,  $w/L = 1/5$  and  $c/H = 0.5$ . As seen from the figures, single circulation cell is formed inside the cavity with clockwise direction. Flow strength decreases with decreasing Grashof number. Comparison of other figure shows that higher flow strength is formed with the increasing of Reynolds number.

Fig. 5 shows the isotherms and streamlines for different values of Grashof numbers. As seen from the figure, variation of Grashof number for  $Gr = 10^3$  and  $10^4$ , temperature distribution and flow field become almost same due to conduction mode of heat transfer. The isotherms move toward to moving lid due to moving flow. Completely different flow field

and isotherms distribution is observed inside the cavity for  $x_L/L = 4/5$  and  $c/H = 0.5$  as seen in Fig. 6. At the lowest value of Grashof number, isotherms are nearly parallel to the heater caused by the domination of conduction mode. However, multiple cells are formed inside the cavity with increasing of Grashof numbers. A cell elongated with vertical wall and that turns in clockwise direction and counterclockwise circulation is formed at the middle of the cavity. Isotherms are nearly parallel to vertical walls. Effects of Reynolds number can be seen on fluid flow and heat for the parameters with  $Da = 0.001$ ,  $w/L = 1/5$  and  $c/H = 0.5$ ,  $Gr = 10^5$  in Fig. 7. For higher Reynolds number, namely, lower Richardson number,  $Ri = Gr/Re^2$ , forced convection becomes effective inside the cavity and a small circulating cell is formed near the right top side of the cavity. The thermal boundary layer's thickness decreases as a result of increasing of Reynolds number but there is no big difference for

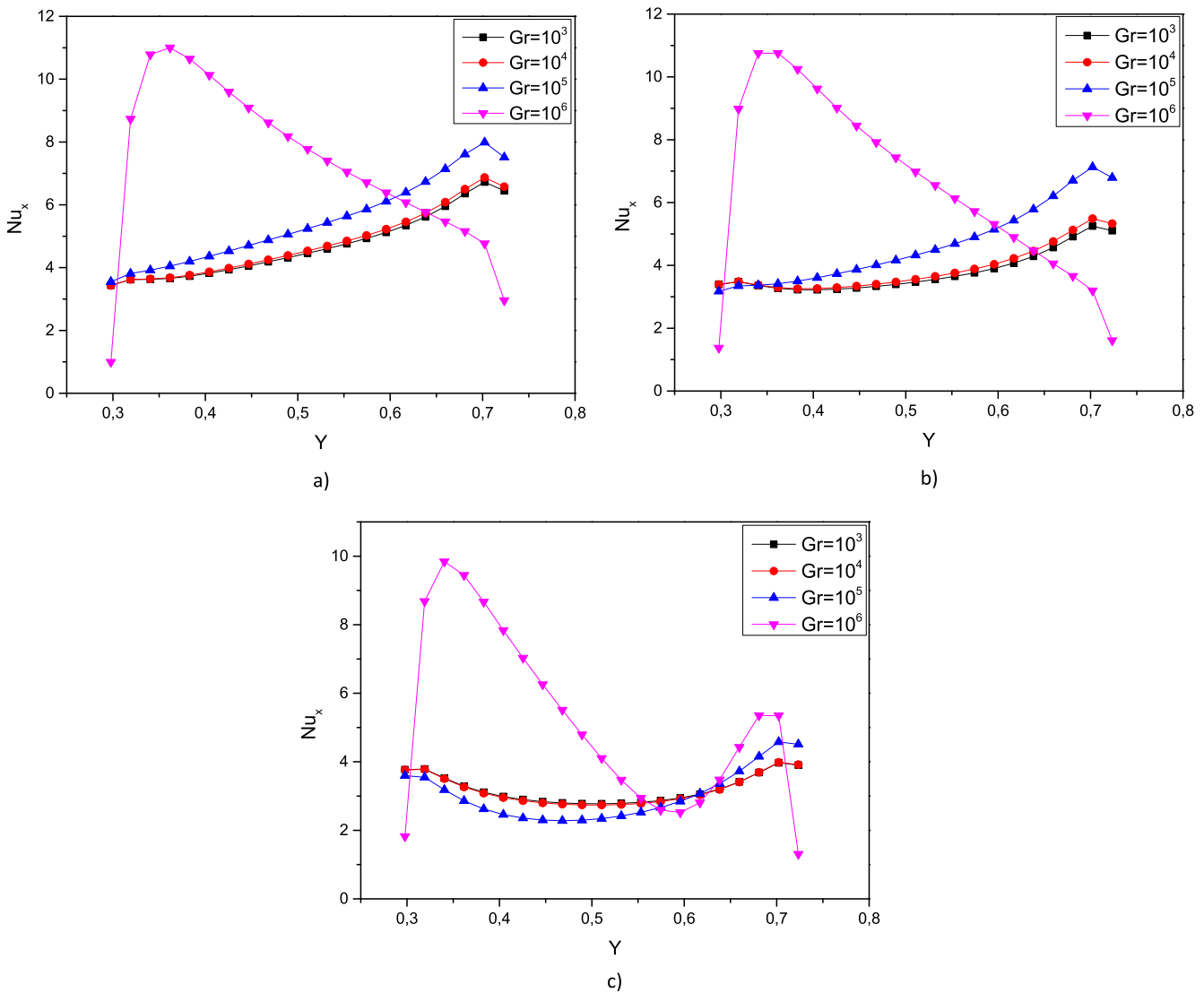
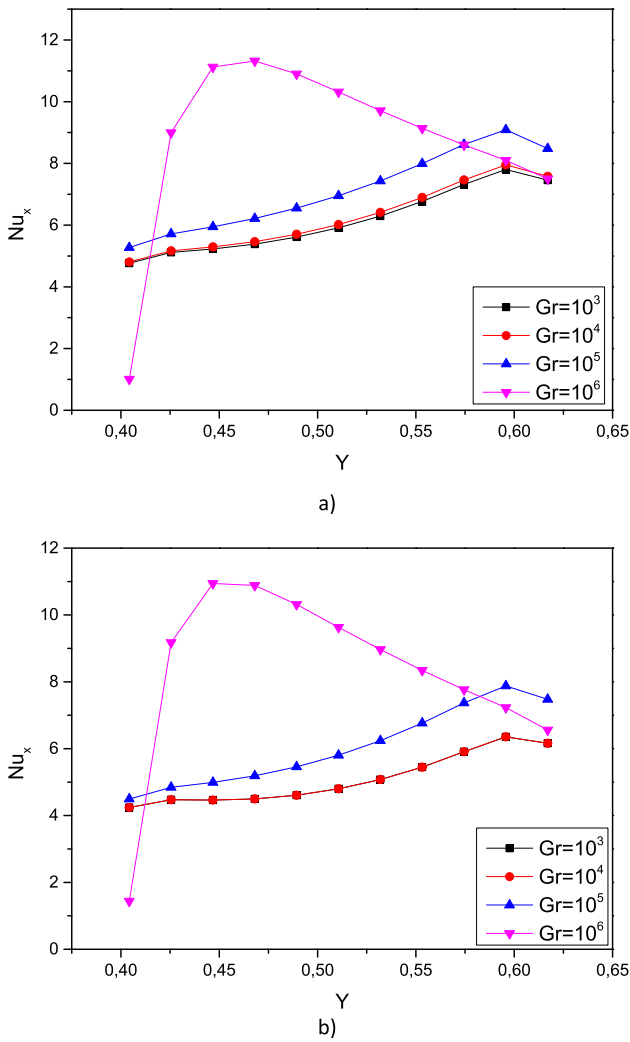


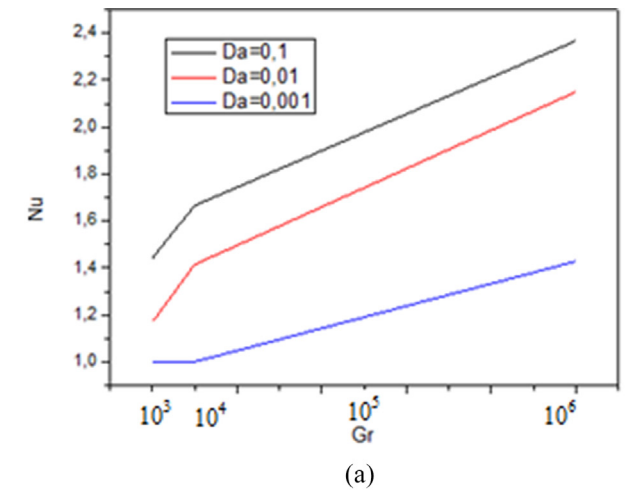
Fig. 9 Variation of local Nusselt number along the heater for different Grashof numbers at  $Re = 100$ ,  $c/H = 0.5$  and  $w/L = 2/5$ , (a)  $Da = 0.1$ , (b)  $Da = 0.01$ , (c)  $Da = 0.001$ .



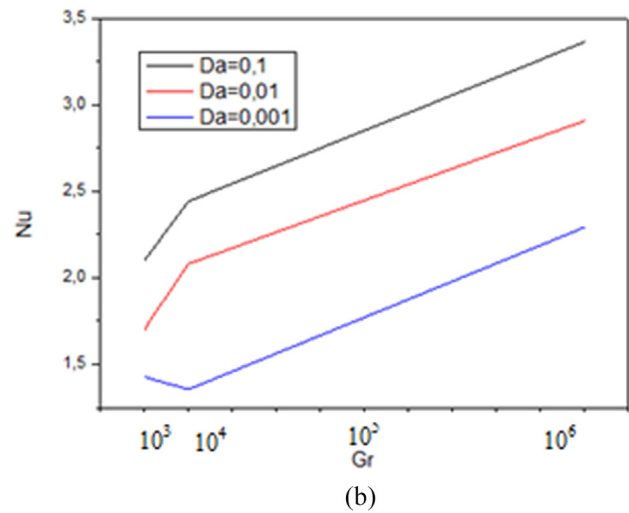
**Fig. 10** Variation of local Nusselt number along the heater for different Grashof numbers at  $Re = 100$ ,  $h/H = 0.5$  and  $w/L = 3/5$  (a)  $Da = 0.1$ , (b)  $Da = 0.01$ .

$Re = 500$  and  $1000$  on flow field. It means that almost similar results can be obtained for further Reynolds number due to domination of forced convection mode of heat transfer. Variation of local Nusselt number are presented in Fig. 8 for  $Re = 100$ ,  $w/L = 1/5$  and  $c/H = 0.5$  at different values of Darcy numbers and Grashof numbers. As seen from the variation of values, heat transfer becomes maximum for  $Gr = 10^6$  because of the convection mode domination for  $Da = 0.1$ . But it declines with increasing the heater length. When, conduction mode of heat transfer becomes dominant, namely, lower values of Grashof number, heat transfer increases along the heater. For this results, local Nusselt number shows a different behavior for  $Gr = 10^4$ , namely, it shows a minimal values around  $Y = 0.6$ . Heat transfer decreases as Darcy numbers decrease. For the highest value of Darcy number, U-shaped distribution is observed for  $Gr = 10^6$ .

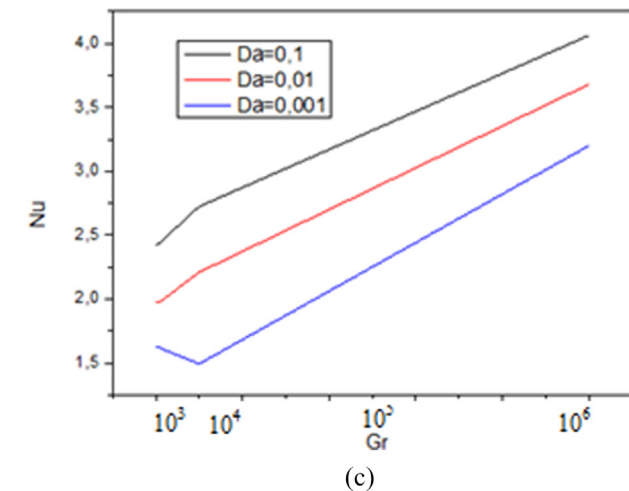
Fig. 9 presents the variation of local Nusselt number for  $Re = 100$ ,  $w/L = 2/5$  and  $c/H = 0.5$  at different Grashof numbers and Darcy numbers. As seen from the figure, there is a maximum value for  $Gr = 10^6$  around  $X = 0.35$ . Other



(a)



(b)



(c)

**Fig. 11** Variation of mean Nusselt number for different parameters, (a)  $w/L = 1/5$ , (b)  $w/L = 2/5$ , (c)  $w/L = 4/5$ .

values of Grashof numbers, local Nusselt numbers are increased along the heater at  $Da = 0.1$ . Results are very similar for  $Da = 0.01$  and variation of local Nusselt numbers exhi-

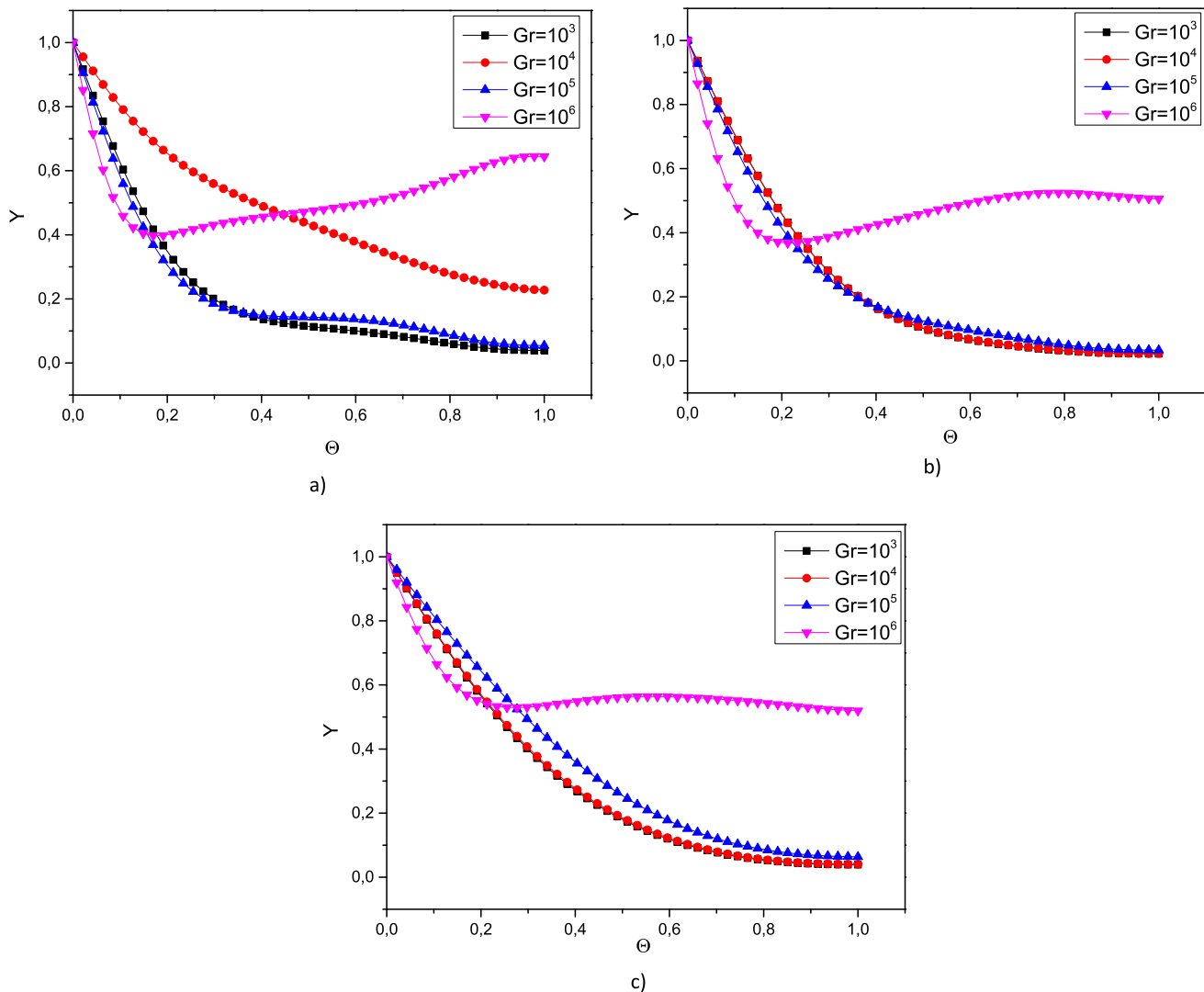


**Fig. 12** Variation of temperature profile at the middle of the cavity for different Grashof numbers at  $Re = 100$ ,  $c/H = 0.5$  and  $w/L =$  (a)  $Da = 0.1$ , (b)  $Da = 0.01$ , (c)  $Da = 0.001$ .

bit same trends. On the contrary, sinewave shaped distribution is obtained for  $Gr = 10^6$  but there is almost constant variation is formed for remaining values of Grashof numbers.

The Fig. 10 shows the variation of local Nusselt numbers for different parameters. As seen from the figure, variation of local Nusselt numbers exhibit similar trends for all values of Darcy numbers but their values are decreased with decreasing of Darcy numbers. Fig. 11 illustrates the variation of mean Nusselt number at different length of heater and different governing parameters such as Grashof and Darcy numbers. As seen from the result that there is a linear increasing with Grashof number and Variation of temperature profile along the heater for different Grashof numbers at different Darcy numbers and  $Re = 100$ ,  $c/H = 0.5$  and  $w/L = 3/5$  is presented in Fig. 12. The trends of temperature profiles give very similar

result for  $Ra \leq 10^5$ . On the contrary, convection heat transfer is occurred for  $Ra = 10^6$  and there is a minimal point around  $Y = 0.4$  and  $0.5$  depending on the Darcy number. It is shown that temperature values of minimum point for  $Ra = 10^6$  is decreased with decreasing of Darcy number. In similar way, Fig. 13 illustrates the variation of temperature profile at the middle of the cavity for different Grashof numbers and Darcy numbers for  $Re = 100$ ,  $c/H = 0.5$  and  $w/L = 2/5$ . Fig. 14 illustrates the variation of temperature with the same parameters of Fig. 13 but for the highest value of heater length. As seen clearly from the figure, temperature values are decreased from the heater to top side of the cavity. When the Grashof number is at its highest value, the curve is more parallel to moving lid which shows the heat transfer's convection mode domination.

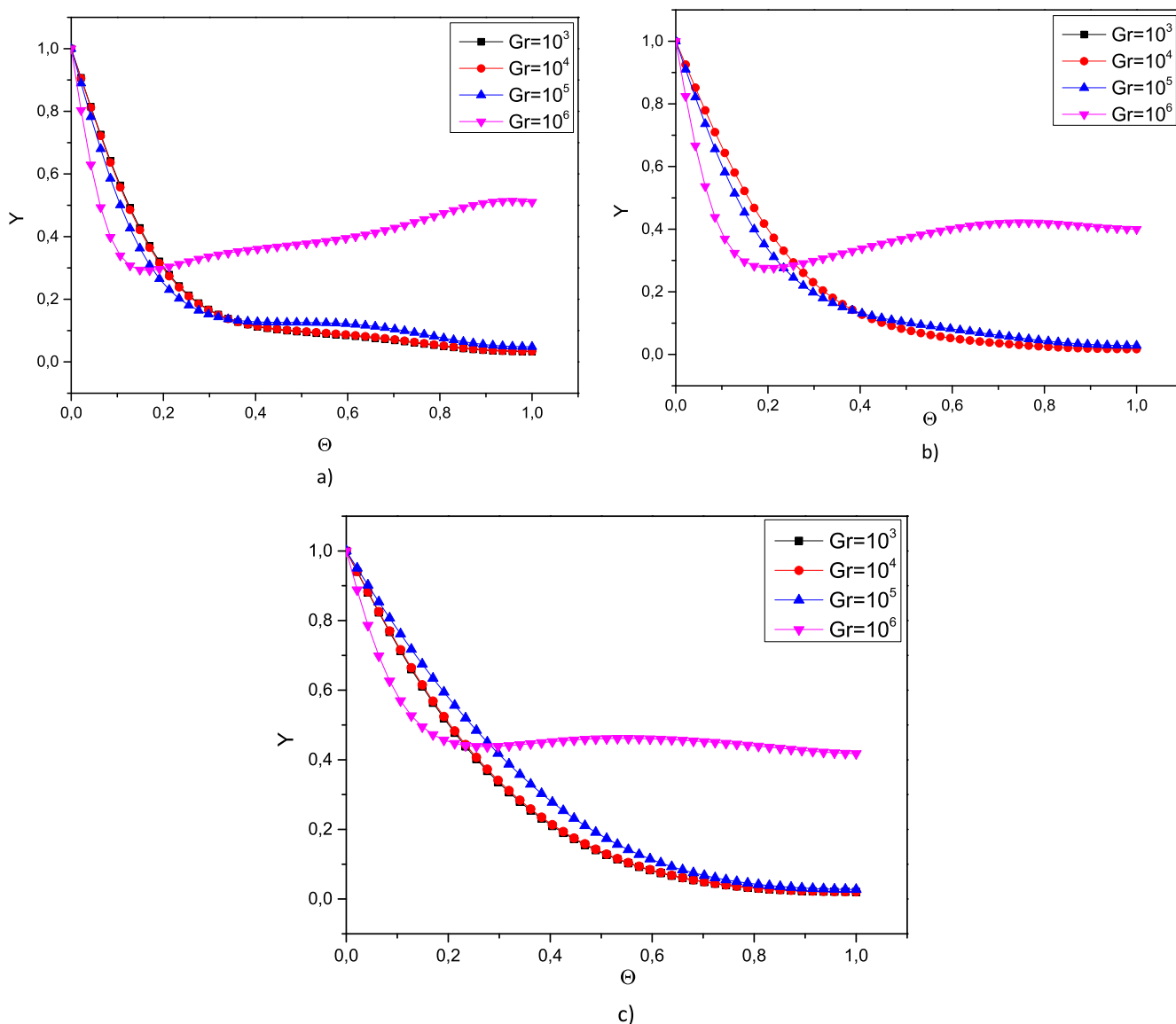


**Fig. 13** Variation of temperature profile at the middle of the cavity for different Grashof numbers at  $Re = 100$ ,  $h/H = 0.5$  and  $w/L = 2/5$  (a)  $Da = 0.1$ , (b)  $Da = 0.01$ , (c)  $Da = 0.001$ .

## 5. Conclusions

A computational work has been performed to investigate the mixed convection in a partially heated lid-driven porous media filled enclosure with one side opening and partial heating. It is clearly seen from the obtained result that flow field and temperature distribution inside the cavity is really complex due to both moving lid and opening side of the cavity. Also, another force comes from the partial heater. Convection mode of heat transfer becomes stronger for higher values of Grashof number and increasing of heater length.

## Declaration of Competing Interest

The authors declare that they have no known competing financial interests or personal relationships that could have appeared to influence the work reported in this paper.

## Acknowledgment

“This project was funded by the Deanship of Scientific Research (DSR), King Abdulaziz University, Jeddah, Saudi Arabia under grant no. (KEP-4-135-38). The authors, therefore, acknowledge with thanks DSR technical and financial support.”

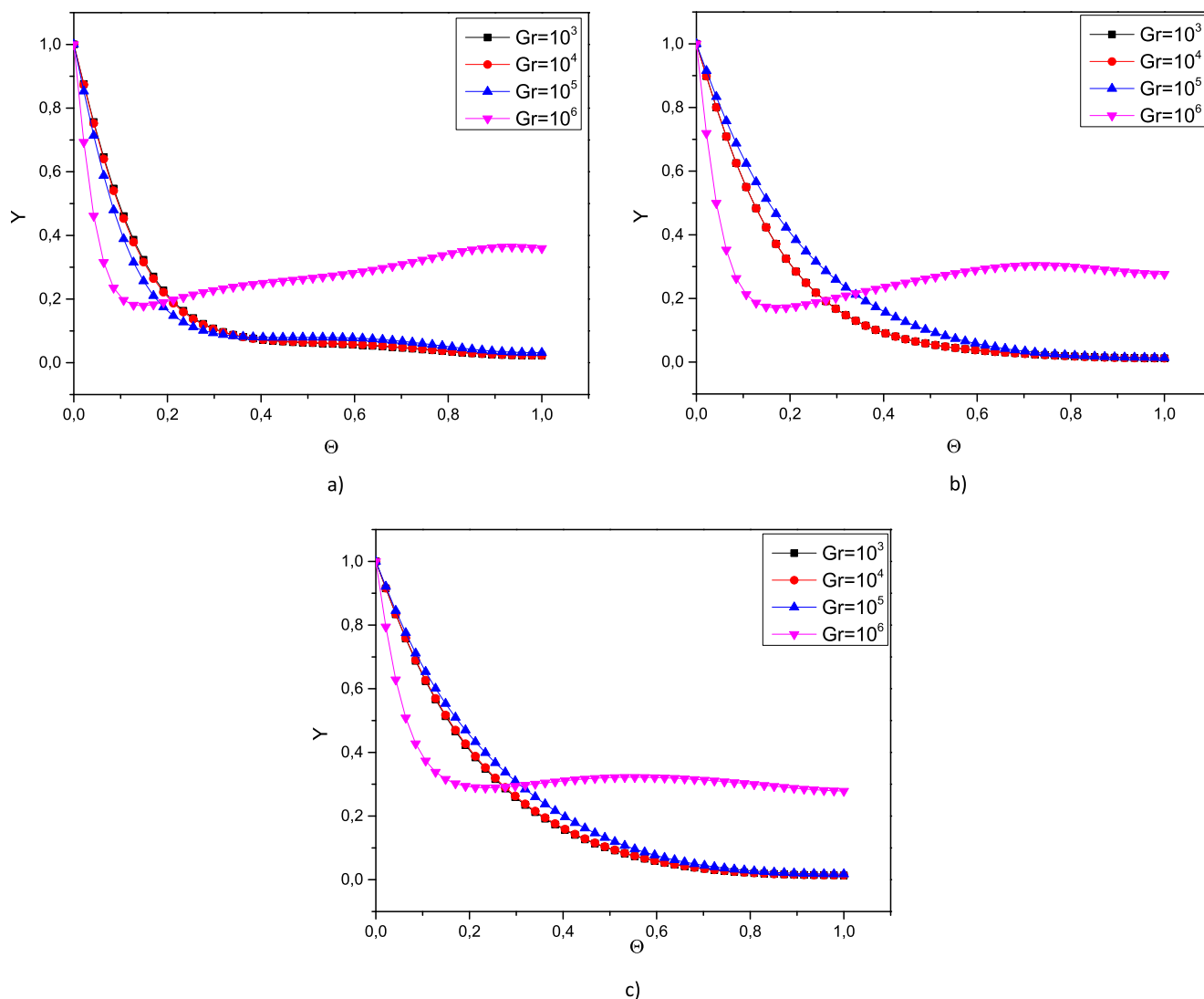


**Fig. 14** Variation of temperature profile at the middle of the cavity for different Grashof numbers at  $Re = 100$ ,  $h/H = 0.5$  and  $w/L = 3/5$  (a)  $Da = 0.1$ , (b)  $Da = 0.01$ , (c)  $Da = 0.001$ .

## References

- [1] D. Ingham, I. Pop, *Transport Phenomena in Porous Media III*, Elsevier, Oxford, 2005.
- [2] D. Nield, A. Bejan, *Convection in Porous Media*, third ed., Springer, NY, 2006.
- [3] P. Vadasz, *Emerging Topics in Heat and Mass Transfer in Porous Media*, Springer, New York, 2008.
- [4] H.F. Öztop, P. Estellé, W.M. Yan, K. Al-Salem, J. Orfi, O. Mahian, A brief review of natural convection in enclosures under localized heating with and without nanofluids, *Int. Commun. Heat Mass Transf.* 60 (2015) 37–44.
- [5] S. Ahmed, H. Öztop, K. Al-Salem, Natural convection coupled with radiation heat transfer in an inclined porous cavity with corner heater, *Comput. Fluids* 102 (2014) 74–84.
- [6] H.F. Öztop, K. Al-Salem, Y. Varol, I. Pop, Natural Convection Heat transfer in a Partially Opened Cavity filled with Porous Media, *Int. J. Heat Mass Transf.* 54 (2011) 2253–2261.
- [7] S. Chung, K. Vafai, Vibration induced mixed convection in an open-ended obstructed cavity, *Int. J. Heat Mass Transf.* 53 (2010) 2703–2714.
- [8] N. Biswas, N.K. Manna, Enhanced convective heat transfer in lid-driven porous cavity with aspiration, *Int. J. Heat Mass Transf.* 114 (2017) 430–452.
- [9] H.F. Öztop, Combined convection heat transfer in a porous lid-driven enclosure due to heater with finite length, *Int. Commun. Heat Mass Transf.* 33 (2006) 772–779.
- [10] D.K. Singh, S.N. Singh, Conjugate free convection with surface radiation in open top cavity, *Int. J. Heat Mass Transf.* 89 (2015) 444–453.
- [11] K. Khanafer, K. Vafai, Effective boundary conditions for buoyancy-driven flows and heat transfer in fully open-ended two-dimensional enclosures, *Int. J. Heat Mass Transf.* 45 (2002) 2527–2538.
- [12] K. Khanafer, K. Vafai, M. Lightstone, Mixed convection heat transfer in two-dimension open-ended enclosure, *Int. J. Heat Mass Transf.* 45 (2002) 5171–5190.
- [13] R. Gutt, T. Grosan, On the lid-driven problem in a porous cavity. A theoretical and numerical approach, *Appl. Math. Comput.* 266 (2015) 1070–1082.
- [14] M. Shekholeslami, M. Shamlooei, Convective flow of nanofluid inside a lid driven porous cavity using CVFEM, *Phys. B* 521 (2017) 239–250.



- [15] A. Chattopadhyaya, S.K. Pandit, A pecllet number based analysis of mixed convection for lid driven porous trapezoidal enclosure, *Procedia Eng.* 127 (2015) 628–635.
- [16] A.M. Al-Amiri, Analysis of momentum and energy transfer in a lid-driven cavity filled with a porous medium, *Int. J. Heat Mass Transf.* 43 (2000) 3513–3527.
- [17] T. Basak, S. Roy, S.K. Singh, I. Pop, Analysis of mixed convection in a lid-driven porous square cavity with linearly heated side wall(s), *Int. J. Heat Mass Transf.* 53 (2010) 1819–1840.
- [18] H.F. Oztop, Natural convection in partially cooled and inclined porous rectangular enclosures, *Int. J. Thermal Sci.* 46 (2007) 149–156.
- [19] S. Chen, W. Gong, Y. Yan, Conjugate natural convection heat transfer in an open-ended square cavity partially filled with porous media, *Int. J. Heat Mass Transf.* 124 (2018) 368–380.
- [20] N. Biswas, N.K. Manna, P. Datta, P.S. Mahapatra, Analysis of heat transfer and pumping power for bottom-heated porous cavity saturated with Cu-water nanofluid, *Powder Technol.* 326 (2018) 356–369.
- [21] W. Shi, K. Vafai, Mixed convection in an obstructed open-ended cavity, *Numer. Heat Transf. J.* 57 (2010) 709–729.
- [22] K. Khanafer, K. Vafai, Double-diffusive mixed convection in a lid-driven enclosure filled with a fluid-saturated porous medium, *Numer. Heat Transf. J.* 42 (2002) 465–486.
- [23] M. Sheikholeslami, Influence of magnetic field on nanofluid free convection in an open porous cavity by means of Lattice Boltzmann method, *J. Mol. Liq.* 234 (2017) 364–374.
- [24] S.E. Ahmed, Mixed convection in thermally anisotropic non-Darcy porous medium in double lid-driven cavity using Bejan's heatlines, *Alexandria Eng. J.* 55 (2016) 299–309.
- [25] M. Rajarathinam, N. Nithyadevi, A.J. Chamkha, Heat transfer enhancement of mixed convection in an inclined porous cavity using Cu-water nanofluid, *Adv. Powder Technol.* 29 (2018) 590–605.
- [26] T. Basak, S. Roy, A.J. Chamkha, A Peclet number based analysis of mixed convection for lid-driven porous square cavities with various heating of bottom wall, *Int. Commun. Heat Mass Transf.* 39 (2012) 657–664.
- [27] S.V. Patankar, *Numerical Heat Transfer and Fluid Flow*, Hemisphere, New York, 1980.
- [28] A. Nakayama, *PC-Aided Numerical Heat Transfer and Convective Flow*, CRC Press, Boca Raton, FL, 1995.
- [29] A. Kasaeian, R. Daneshzarian, O. Mahian, L. Kolsi, A.J. Chamkha, S. Wongwises, I. Pop, Nanofluid flow and heat transfer in porous media: a review of the latest developments, *Int. J. Heat Mass Transf.* 107 (2017) 778–791.
- [30] S.E. Ahmed, A.K. Hussein, H.A. Mohammed, I.K. Adegund, X. Zhange, L. Kolsi, A. Hasanpour, S. Sivasankaranh, Viscous dissipation and radiation effects on MHD natural convection in a square enclosure filled with a porous medium, *Nucl. Eng. Des.* 266 (2014) 34–42.
- [31] K.M. Khanafer, A.J. Chamkha, *Int. J. Heat Mass Transf.* 42 (1999) 2465–2481.
- [32] A.J. Chamkha, Double-diffusive convection in a porous enclosure with cooperating temperature and concentration gradients and heat generation or absorption effects, *Numer. Heat Transf.: Part A: Appl.* 41 (1) (2002) 65–87.
- [33] A. Haghshenas, M.R. Nasr, M.H. Rahimian, Numerical simulation of natural convection in an open square cavity filled with porous medium by lattice Boltzmann method, *Int. Comm. Heat Mass Transfer* (2010).
- [34] H. Oztop, E. Bilgen, Natural convection in differentially heated and partially divided square cavities with internal heat generation, *Int. J. Heat Fluid Flow* 27 (2006) 466–475.
- [35] A.C. Baytas, Entropy generation for natural convection in an inclined porous cavity, *Int. J. Heat Mass Transf.* 43 (2000) 2089–2099.
- [36] N.H. Saeid, I. Pop, Transient free convection in a square cavity filled with a porous medium, *Int. J. Heat Mass Transf.* 47 (2004) 1917–1924.
- [37] U. Ghia, K.N. Ghia, C.T. Shin, High-Re Solutions for incompressible flow using the Navier-Stokes equations and multigrid method, *J. Comput. Phys.* 48 (1982) 387–411.
- [38] K. Al-Salem, H.F. Oztop, I. Pop, Y. Varol, Effects of moving lid direction on MHD mixed convection in a linearly heated cavity, *Int. J. Heat Mass Transf.* 55 (2012) 1103–1112.